

The role of interfacial friction on the peeling of thin viscoelastic tapes

M. Ceglie,¹ N. Menga,^{1,2,*} and G. Carbone^{1,2}

¹*Department of Mechanics, Mathematics and Management,
Politecnico of Bari, V.le Japigia, 182, 70126, Bari, Italy*

²*Imperial College London, Department of Mechanical Engineering,
Exhibition Road, London SW7 2AZ*

Abstract

We study the peeling process of a thin viscoelastic tape from a rigid substrate. Two different boundary conditions are considered at the interface between the tape and the substrate: stuck adhesion, and relative sliding in the presence of frictional shear stress. In the case of perfectly sticking interfaces, we found that the viscoelastic peeling behavior resembles the classical Kendall behavior of elastic tapes, with the elastic modulus given by the tape high-frequency viscoelastic modulus. Including the effect of frictional sliding, which occurs at the interface adjacent to the peeling front, makes the peeling behavior strongly dependent on the peeling velocity. Also, at sufficiently small peeling angles, we predict a tougher peeling behavior than the classical stuck cases. This phenomenon is in agreement with recent experimental evidences indicating that several biological systems (e.g. geckos, spiders) exploit low-angle peeling to control attachment force and locomotion.

Keywords: peeling, viscoelasticity, interfacial friction, adhesion

arXiv:2109.04782v2 [cond-mat.soft] 15 Nov 2021

*Electronic address: nicola.menga@poliba.it

I. INTRODUCTION

The ability to control the mechanical behavior of real interfaces is one of the most challenging topic in modern industrial engineering, as witnessed by the effort made in the last decades in elastic [1–8], viscoelastic [9–16] and adhesive [17–24] contact mechanics studies. In this respect, the functionality of several real-life devices such as, for instance, pressure sensitive adhesives, modern touch screens, biomedical wound dressing and Band-Aids, is tightly connected to the possibility of tailoring the interfacial adhesion between these systems and the mating surfaces. Therefore, the attachment/detachment performances of such interfaces are of primary concern. Among the possible detachment mechanisms, peeling is usually regarded as one of the most important [25] as it offers the chance to independently variate both the peeling load P and the peeling angle θ . Due to its reliability, also the adhesive performance of industrial interfaces is often controlled by means of opportunely designed peeling tests [26]. For these reasons, a deep understanding of the physics behind peeling processes is of primary importance in modern engineering.

The basic understanding of the peeling behavior of thin elastic tapes is nowadays well established. Indeed, Kendall's [27] studies set the theoretical framework to investigate the peeling evolution by relying on energy balance of the system. His pioneering results were valid under specific hypothesis, such as the linear elasticity of the tape, perfect interfacial backing between the tape and the substrate. However, in the last decades, most of the original assumptions have been relaxed in successive studies. This is the case, for instance, of the effect of bending stiffness in thick tapes, which has been investigated in Refs [28, 29] in the presence of viscous losses occurring in the adhesive layer and in the tape. In Refs [30, 31], the effect of the substrate viscoelasticity on the peeling behavior has been studied to show that the steady detachment speed can be tuned under specific conditions and ultra-tough peeling may occur at low peeling angles. The effect of the tape viscoelasticity has been investigated in Ref. [32–35], where it has been empirically shown that, in a limited range of peeling velocities [25], the peeling force $P \approx kV^n$.

Also the tape-substrate interfacial interactions play a fundamental role in determining the evolution of the peeling process. Kendall showed that interfacial sliding between the tape and the substrate may trigger cyclic detachment and re-attachment of the tape [36, 37]. Nonetheless, such a relative sliding represents an additional source of energy dissipation due to frictional shear stress occurring at the interface [38, 39]. This has been investigated in details in the case of elastic tapes peeled away from rigid substrates under frictionless [40] and frictional [41] sliding. Theoretical and experimental investigations have concluded that, as expected, the presence of frictional sliding at the interface leads to significantly higher peeling force, which may theoretically diverge at vanishing peeling angle. It has been suggested that the enhancement of peeling force caused by the energy dissipated in frictional sliding plays a key role in biological applications. Indeed, several studies have identified this mechanism as one of the possible sources of the superior adhesive performance and the ability to switch between firm attachment and effortless detachment of geckos [42–44], insects [45, 46] and frogs [47], together with the hierarchical configuration of the pad/toes fibrils [48–50], and the V-shaped peeling scheme often occurring at the interface [51–54]. Specifically, in the presence of interfacial sliding, the enhanced peeling force arises due to the combination of three main physical mechanisms [55]: (i) tape pre-strain due to partial sliding occurring during detachment [56, 57]; (ii) the friction losses associated with the slip at the interface [58]; (iii) the viscous dissipation [46]. Interestingly, in wet contact case, the

last contribution is usually ascribed to the viscous shear in the interfacial thin fluid film formed by the pad secretion [59, 60]; however, a comprehensive model on the effect of the pad tissue bulk viscoelasticity [61, 62] on the overall frictional peeling is lacking.

In this study, we present a theoretical model of the behavior of a thin viscoelastic tape peeled away from a rigid substrate. Specifically, we aim at investigating the combined effect of frictional interfacial sliding occurring during the detachment process and the energy dissipation associated with the viscoelastic behavior of the tape. In order to shed light on the interplay between these mechanisms of energy dissipation, we consider two different configurations: (i) firstly, we focus on stuck conditions, where a rigid constraint avoids any possible interfacial displacement between the tape and the substrate, so that no additional energy contribution is present at interface beside the change in the energy of adhesion; then (ii) we consider the sliding case, where energy dissipation occurs due to frictional relative sliding in the tape elongated region. Our findings may be of help to estimate the effect of the bulk viscoelasticity on the overall peeling behavior of bioinspired and natural systems (e.g. biological fibrils, industrial polymeric tapes, etc.) in the presence of interfacial frictional sliding.

II. FORMULATION

In this section, we present the mathematical model for the viscoelastic peeling assuming two different conditions at the interface between the tape and the rigid substrate: (i) stuck adhesion, where tape normal and tangential displacements are inhibited; (ii) relative frictional sliding, i.e. tape normal displacements are inhibited but tangential sliding occurs, which is opposed by frictional shear stresses. In both cases, the problem formulation builds on energy balance. We focus on a linear viscoelastic material with a single relaxation time t_c . Further, we neglect any dynamic effect during the tape detaching process (*i.e.* we assume that the peeling front velocity is steady and far lower than the speed of sound in the tape).

Stuck interface

Consider a viscoelastic tape of thickness d and transverse width b , baked onto a rigid substrate with no relative sliding at the interface. As shown in Fig. 1, the tape is peeled away at an angle θ under a constant force P . We assume the peeling front moves on the left at a constant velocity V_0 relative to the substrate. We observe the peeling process in the peeling front, so that the substrate moves on the right at speed V_0 as shown in Fig. 1.

Under steady state conditions, the energy balance per unit time of the viscoelastic tape is given by

$$W_E + W_I + W_S = 0 \quad (1)$$

where W_E is the work per unit time of the external forces acting on the tape, W_I is work per unit time done by tape internal stresses, which takes into account for both the change in the stored elastic and viscous energy dissipation in the tape, and W_S is the work per unit time done by interfacial forces. Notably, in this formulation we neglect any other source of energy dissipation, such as acoustic or thermal emissions.

The term W_E in Eq. (1) can be calculated considering the external forces acting on the system, which are the remote load P acting on the detached tape tip, and the corresponding

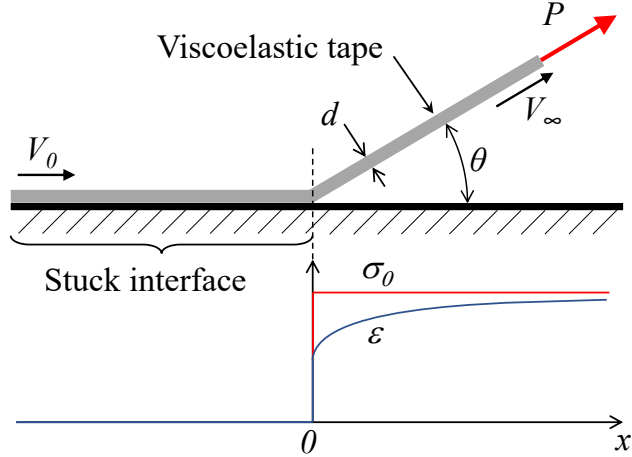


FIG. 1: The scheme of the peeling process of a thin viscoelastic layer from a rigid substrate in the presence of stuck adhesion at the interface, so that no relative sliding occurs. In the lower part, qualitative diagrams of the tape stress σ (red) and deformation ε (blue) are shown.

opposite substrate reaction force $-P \cos \theta$. We have

$$W_E = PV_\infty - PV_0 \cos \theta = \sigma_0 V_0 b d \left(1 + \frac{\sigma_0}{E_0} - \cos \theta \right) \quad (2)$$

where we defined $\sigma_0 = P/bd$, and E_0 is the low frequency viscoelastic modulus. Moreover, the mass balance of the tape gives $V_\infty = V_0(1 + \sigma_0/E_0)$. Notably, in Eq. (2) we assumed that the tape tip (where the force P is applied) is located sufficiently far from the peeling front, so that complete viscoelastic relaxation occurs in the detached tape.

The surface term W_S in Eq. (1) represents the energy per unit time associated with the rupture of interfacial adhesive bond, with $\Delta\gamma$ being the work of adhesion needed to detach a unit surface of the tape from the substrate. Although $\Delta\gamma$ may also depend on the viscoelastic energy dissipation occurring very close to the crack tip (i.e. small-scale viscoelasticity), for the sake of simplicity, here we neglect such effects, thus assuming a constant $\Delta\gamma$ value. Nonetheless, this effect could be straightforwardly introduced in the present model by opportunely modifying the value of $\Delta\gamma$ as described in Refs. [63, 64]. Therefore, we can write

$$W_S = -\Delta\gamma b V_0 \quad (3)$$

As mentioned above, the term W_I in Eq. (1) takes into account for both the elastic energy stored in the tape, and the bulk energy dissipation occurring due to viscoelastic creep in the detached strip. Moreover, observing that the bending stiffness of the tape depends on the third power of thickness d , and considering that we focus on very thin tapes, the bending contribution to W_I can be neglected (see also Refs. [52, 53]). Hence we write

$$W_I = -V_0 b d \int_{-\infty}^{+\infty} \sigma(x) \dot{\varepsilon}(x) dx \quad (4)$$

where $\dot{\varepsilon}(x)$ is the spatial derivative of the strain $\varepsilon(x)$. Note that, in Eq. (4), we used $\dot{\varepsilon}(x) = V_0 \varepsilon'(x)$, with $\dot{\varepsilon}(x)$ being the time derivative of $\varepsilon(x)$.

Since in this section we assume no interfacial sliding between the adhering tape and the rigid substrate, the stress distribution in the viscoelastic tape is given by $\sigma(x) = \sigma_0 H(x)$, with $H(x)$ being the Heaviside step function (see the diagram in Fig. 1). Moving from the linear viscoelastic constitutive equation [65], in the framework of steady state conditions, the deformation field can be calculated as

$$\varepsilon(x) = \int_{-\infty}^x J(x-s)\sigma'(s) ds \quad (5)$$

where $J(x)$ is the spatial transformation of the viscoelastic creep function given by

$$J(x) = H(x) \left[\frac{1}{E_0} - \frac{1}{E_1} \exp\left(-\frac{x}{\lambda}\right) \right] \quad (6)$$

where $\lambda = V_0 t_c$ is the relaxation length, and $E_1^{-1} = E_0^{-1} - E_\infty^{-1}$ with E_0 and E_∞ being the low and very high frequency viscoelastic moduli, respectively.

For the case at hand, Eq. (5) gives $\varepsilon(x) = \sigma_0 J(x)$, which substituting into Eq. (4), after some algebra, gives

$$W_I = -V_0 b d \sigma_0^2 \left(\frac{1}{E_0} - \frac{1}{2E_\infty} \right) = -\frac{V_0 b d \sigma_0^2}{2} \left(\frac{1}{E_0} + \frac{1}{E_1} \right) \quad (7)$$

where we used $\int_{-\infty}^{+\infty} \delta(x) H(x) dx = 1/2$, which gives $\varepsilon(0) = \frac{1}{2} [\varepsilon(0^-) + \varepsilon(0^+)] = \frac{1}{2} \varepsilon(0^+)$. Note that the viscoelastic dissipated energy per unit time is

$$D_s = \frac{V_0 b d \sigma_0^2}{2E_1} \quad (8)$$

Finally, substituting Eqs. (2,3,7) into Eq. (1) we have

$$\frac{\sigma_0^2}{2E_\infty} + \sigma_0(1 - \cos \theta) = \frac{\Delta\gamma}{d} \quad (9)$$

which represents the peeling equilibrium condition. Interestingly regardless of the peeling velocity V_0 , Eq. (9) is identical to the Kendall equation with the elastic modulus given by the high frequency viscoelastic modulus E_∞ . Notice that Eq. (9) can be rephrased as

$$\frac{1}{2} \left(\frac{\sigma_0}{E_0} \right)^2 + \kappa \frac{\sigma_0}{E_0} (1 - \cos \theta) = \kappa \frac{\Delta\gamma}{E_0 d} \quad (10)$$

where we have defined $\kappa = E_\infty/E_0$. For $\theta = 0$, we get

$$\sigma_K = \sqrt{\frac{2\kappa E_0 \Delta\gamma}{d}} = \sqrt{\frac{2E_\infty \Delta\gamma}{d}} \quad (11)$$

so that, in this case, the peeling is much more tough than in the (low frequency) elastic case as the effective work of adhesion is κ -times larger than $\Delta\gamma$.

In order to explain the appearance of the high-frequency viscoelastic modulus E_∞ in Eq. (9) we note that, because of the stuck condition assumption (no relative sliding at the tape-substrate interface), the tape is subjected to an abrupt stretching in the peeling section (see

Fig. 1). For this reason, regardless of the peeling velocity V_0 , the material response close to the peeling front is governed by the high-frequency viscoelastic response, which makes the tape locally behave as a perfectly elastic material with elastic modulus E_∞ .

Notably, in real conditions, the abrupt change of the tape stress during peeling would be smoothed, as it must occur on a finite length scale across the peeling section. Since the size of this "process zone" can be estimated of order unity of the tape thickness d (see also Refs [52, 66]), the tape excitation frequency during peeling is $\omega \approx V_0/d$, so that at very low peeling velocities, i.e. when $V_0 \ll d/t_c$, the tape response would be governed by the low-frequency viscoelastic modulus E_0 . However, since we usually expect that $V_0 \gg d/t_c$, this would not qualitatively affect the physical picture of the peeling behavior provided so far.

Frictional sliding interface

The discussion provided in the previous section is based on the assumption that the tape firmly sticks to the rigid substrate, and the tangential component of the peeling force P , remotely acting on the tape tip, is locally balanced by a point reaction force acting in the peeling section. However, it has been shown that a certain amount of relative sliding occurs in real interfaces [38, 58, 67], so that the tangential component of the peeling force P is balanced by the frictional shear stresses arising at the interface between the tape and the rigid substrate. In this case, assuming a uniform interfacial shear stress τ , a portion of the adhering tape of length $a = P \cos \theta / \tau b$ is gradually stretched and slides against the substrate. Such a physical scenario is shown in Fig. 2.

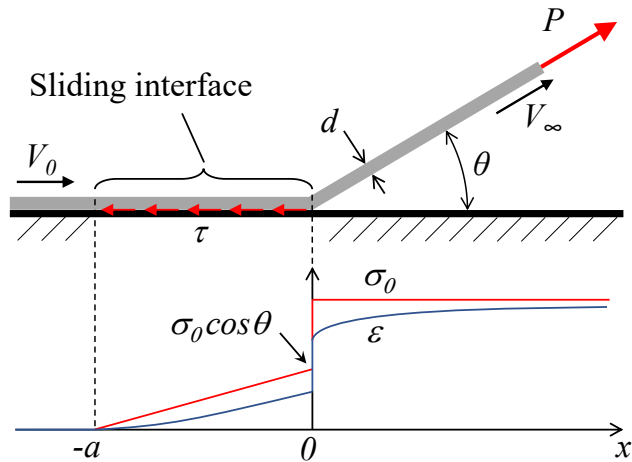


FIG. 2: The scheme of the peeling process of a thin viscoelastic layer from a rigid substrate in the presence of relative sliding at the interface. Notably, τ is the frictional shear stress. In the lower part, qualitative diagrams of the tape stress σ (red) and deformation ε (blue) are shown.

The work per unit time done by interfacial frictional stresses is

$$W_T = - \int_{-a}^0 V_S(x) \tau b dx = -\tau b V_0 \int_{-a}^0 \varepsilon(x) dx \quad (12)$$

where $V_S(x) = V_0\varepsilon(x)$ is the sliding velocity distribution at the interface. Of course, both the stress and deformation distributions along the tape are modified due to the presence of the tangential tractions τ . Indeed, we have

$$\begin{aligned}\sigma(x) &= \frac{\tau}{d}(x+a); & -a \leq x < 0 \\ \sigma(x) &= \sigma_0; & x > 0\end{aligned}\quad (13)$$

where $\sigma_0 \cos\theta = \tau a/d$. Similarly, from Eq. (13), recalling, Eq. (5), one obtains

$$\begin{aligned}\varepsilon(x) &= \frac{\tau}{E_0 d}(a+x) - \frac{\tau\lambda}{E_1 d} \left[1 - \exp\left(-\frac{x+a}{\lambda}\right) \right]; & -a \leq x < 0 \\ \varepsilon(x) &= \frac{\sigma_0}{E_0} - \frac{\sigma_0}{E_1} \left\{ 1 - \frac{\tau a}{\sigma_0 d} + \frac{\tau\lambda}{\sigma_0 d} \left[1 - \exp\left(-\frac{a}{\lambda}\right) \right] \right\} \exp(-x/\lambda); & x > 0\end{aligned}\quad (14)$$

Recalling Eq. (12) and using Eqs. (13, 14) we have

$$W_T = -bdV_0 \frac{\sigma_0^2}{2E_0} \cos^2\theta \left\{ 1 - 2\frac{\kappa-1}{\kappa} \frac{\lambda}{a} \left[1 - \frac{\lambda}{a} + \frac{\lambda}{a} \exp\left(-\frac{a}{\lambda}\right) \right] \right\} \quad (15)$$

In Eq. (15), we note that for $a/\lambda \rightarrow \infty$ we get $W_T \rightarrow -\frac{1}{2}bdV_0(\sigma_0^2/E_0) \cos^2\theta$, which involves the low frequency modulus E_0 ; whereas, for $a/\lambda \rightarrow 0$ we get $W_T \rightarrow -\frac{1}{2}bdV_0(\sigma_0^2/E_\infty) \cos^2\theta$, which involves the high frequency modulus E_∞ . Moreover, $W_T(a/\lambda \rightarrow \infty) = \kappa W_T(a/\lambda \rightarrow 0)$.

This time, the work per unit time done by tape internal stresses is

$$\begin{aligned}W_I &= -bdV_0 \int_{-\infty}^{+\infty} \sigma(x) \varepsilon'(x) dx = \\ &= -bdV_0 \frac{\sigma_0^2}{2E_0} \left(\cos^2\theta \left\{ 1 - 2\frac{\kappa-1}{\kappa} \frac{\lambda}{a} \left[\frac{\lambda}{a} - \left(1 + \frac{\lambda}{a} \right) \exp\left(-\frac{a}{\lambda}\right) \right] \right\} \right. \\ &\quad \left. - \frac{1}{\kappa} (1 - \cos^2\theta) - 2\frac{\kappa-1}{\kappa} \left\{ 1 - \cos\theta \left[1 - \frac{\lambda}{a} + \frac{\lambda}{a} \exp\left(-\frac{a}{\lambda}\right) \right] \right\} \right) \quad (16)\end{aligned}$$

Finally, recalling that, in this case, Eq. (1) modifies in

$$W_E + W_I + W_S + W_T = 0 \quad (17)$$

and using Eqs. (2,3,15,16) into Eq. (17), the final peeling equilibrium equation for a viscoelastic tape in the presence of frictional sliding at the interface is given by

$$\begin{aligned}\frac{\sigma_0^2}{2E_0} \left\{ (1 - \cos^2\theta) - \frac{\kappa-1}{\kappa} (1 - \cos\theta) \left(1 + 2\cos\theta \left[\frac{\lambda}{a} \left(1 - \exp\left(-\frac{a}{\lambda}\right) \right) - \frac{1}{2} \right] \right) \right\} \\ + \sigma_0(1 - \cos\theta) - \frac{\Delta\gamma}{d} = 0\end{aligned}\quad (18)$$

III. NUMERICAL RESULTS

Let us introduce the following dimensionless parameters: $\tilde{\sigma}_0 = \sigma_0/E_0$, $\tilde{\tau} = \tau/E_0$, $\Delta\tilde{\gamma} = \Delta\gamma/(E_0d)$ and $\tilde{V}_0 = V_0t_c/d$. Note that $a/\lambda = \tilde{\sigma}_0 \cos\theta / (\tilde{V}_0\tilde{\tau})$. Therefore, Eq. (18) becomes

$$\frac{1}{2}\tilde{\sigma}_0^2 \left\{ (1 - \cos^2\theta) - \frac{\kappa - 1}{\kappa} (1 - \cos\theta) \left(1 + 2\cos\theta \left[\frac{\tilde{V}_0\tilde{\tau}}{\tilde{\sigma}_0 \cos\theta} \left(1 - \exp\left(-\frac{\tilde{\sigma}_0 \cos\theta}{\tilde{V}_0\tilde{\tau}}\right) \right) - \frac{1}{2} \right] \right) \right\} + \tilde{\sigma}_0(1 - \cos\theta) = \Delta\tilde{\gamma} \quad (19)$$

In the limiting cases of $\tilde{V}_0 \gg 1$ and $\tilde{\tau} \gg 1$, Eq. (18) gives

$$\frac{1}{2} \frac{\sigma_0^2}{E_\infty} (1 - \cos^2\theta) + \sigma_0(1 - \cos\theta) = \frac{\Delta\gamma}{d} \quad (20)$$

which clearly differs from Eq. (9), showing that the energy dissipation due to frictional sliding at the interface is proportional to $\frac{1}{2}(\sigma_0^2/E_\infty)\cos^2\theta$, which leads to much tougher peeling behavior at small peeling angle, as the peeling stress σ_0 diverges as σ_K/θ . This result has been already observed in Refs. [41, 68] for purely elastic tapes (E is replaced by E_∞), and it can be interpreted as the emergence of an infinitely tough peeling behavior. Incidentally, it is worth noticing that ultra-tough peeling has been also predicted to occur when the tape is elastic and the substrate viscoelastic [30, 31].

Similarly, in the limiting case of $\tilde{V}_0\tilde{\tau} \ll 1$ with $\tilde{V}_0 \gg 1$ (i.e. $V_0 \gg d/t_c$), Eq. (18) becomes

$$\frac{1}{2} \frac{\sigma_0^2}{E_0} (1 - \cos^2\theta) - \frac{[\sigma_0(1 - \cos\theta)]^2}{2E_1} + \sigma_0(1 - \cos\theta) = \frac{\Delta\gamma}{d}, \quad (21)$$

where the tape response in the adhered portion subjected to frictional shear stresses is governed by the low frequency viscoelastic modulus E_0 . However, in Eq. (21), the additional term

$$\frac{\sigma_0^2(1 - \cos\theta)^2}{2E_1} = \frac{D_f}{V_0bd} = (1 - \cos\theta)^2 \frac{D_s}{V_0bd} \quad (22)$$

takes into account for the viscoelastic energy dissipation per unit time D_f , triggered by the stress step change $\Delta\sigma = \sigma_0 - \sigma_0 \cos\theta$, which still occurs at the peeling front. Indeed, Eq. (8) is still valid provided that σ_0 is replaced by $\Delta\sigma$. Notice that, as already discussed before, for $\tilde{V}_0 \ll 1$ (i.e. $V_0 \ll d/t_c$) the term D_f must also vanish, as even in the peeling section the tape behaves elastically with modulus E_0 . Therefore, for $\tilde{\tau} \ll 1$ and $\tilde{V}_0 \ll 1$ (i.e. $V_0 \ll d/t_c$), Eq. (18) becomes

$$\frac{1}{2} \frac{\sigma_0^2}{E_0} (1 - \cos^2\theta) + \sigma_0(1 - \cos\theta) = \frac{\Delta\gamma}{d} \quad (23)$$

which holds true for purely elastic tapes (with elastic modulus $E = E_0$) in the presence of interfacial frictional sliding (see Refs [41, 68]).

Figures 3 show the dimensionless peeling stress $\tilde{\sigma}_0$ as a function of the peeling angle θ , for both stuck and sliding interfaces and different values of the parameter $\kappa = E_\infty/E_0$ [Fig. 3a], and of the energy of adhesion $\Delta\gamma$ [Fig. 3b].

As already discussed, in the stuck case (dashed lines in both figures) we recover the well-known elastic Kendall's solution, where the elastic modulus is replaced by the high-frequency

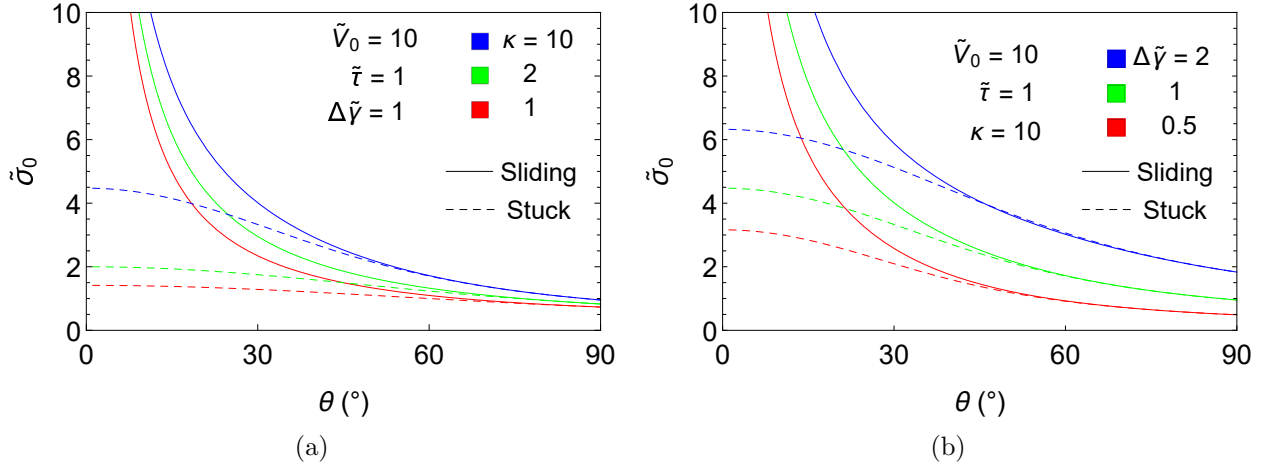


FIG. 3: The dimensionless peeling stress $\tilde{\sigma}_0$ as a function of the peeling angle θ , for different values of (a) the viscoelasticity parameter $\kappa = E_\infty/E_0$; and (b) the dimensionless energy of adhesion $\Delta\tilde{\gamma}$. The dashed curves refer to the case of stuck interface between the tape and the rigid substrate, whereas continuous curves refer to frictionally sliding interfaces.

viscoelastic modulus E_∞ [see Eq. (9)]. Given the values of the low-frequency viscoelastic modulus E_0 , the peeling angle θ and work of adhesion $\Delta\gamma$, the peeling force increases with the parameter $\kappa = E_\infty/E_0$.

On the other hand, in case of frictional sliding at the interface a very different scenario emerges. This time, the peeling process is governed by Eq. (18), which, regardless of the κ value, leads to unbounded peeling forces for vanishing peeling angle θ (see continuous lines in Figures 3a and 3b). In this case, the dimensionless peeling stress obeys the equation $\tilde{\sigma}_0 = \sqrt{2\Delta\tilde{\gamma}}/\theta$ for $\theta \rightarrow 0$. Interestingly, such a result is in agreement with several experimental observations on the peeling behavior of insects pads in the presence of relative frictional sliding between the fibrils and the substrate [43, 55, 67]. Figure 3b presents the effect of the dimensionless energy of adhesion $\Delta\tilde{\gamma}$ on the peeling behavior. As expected, regardless of the specific interface behavior, increasing $\Delta\tilde{\gamma}$ leads to an overall tougher peeling behavior, as the necessary stress $\tilde{\sigma}_0$ to sustain the peeling process increases [27].

Figure 4 shows the dimensionless peeling stress $\tilde{\sigma}_0$ as a function of the peeling angle θ . This time, different values of the dimensionless parameter $\tilde{V}_0\tilde{\tau}$ are considered. In the same figure, we also report the purely elastic solution in the presence of frictional sliding (with elastic modulus $E = E_0$). We observe that, for relatively small values of the parameter $\tilde{V}_0\tilde{\tau}$ (red curve) and moderately large peeling angles θ , the value of $\tilde{\sigma}_0$, observed in presence of frictional sliding, is lower than the value predicted in the case of stuck interface (black dashed curve). This is related to the different mechanisms of energy dissipation occurring in each case. Indeed, for a stuck interface, the only source of energy dissipation arises from the viscoelastic creep occurring in the detached branch of tape (i.e. for $x > 0$), which is independent on θ . On the contrary, when dealing with interfaces where frictional relative motion occurs between the tape and the substrate, two additional sources of energy dissipation can be identified: (i) the work done by the frictional shear stress at the interface; and (ii) the viscoelastic creep occurring in the portion of the tape adhered to the substrate

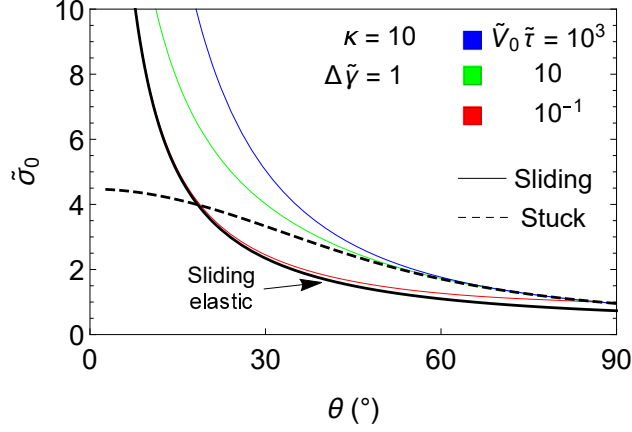


FIG. 4: The dimensionless peeling stress $\tilde{\sigma}_0$ as a function of the peeling angle θ , for different values of the dimensionless parameter $\tilde{V}_0\tilde{\tau}$. The dashed curve refers to the case of stuck interface between the tape and the rigid substrate, whereas continuous curves refer to frictionally sliding interfaces. In the same figure, we also plot for comparison the peeling behavior of an elastic tape in frictional sliding. Results refer to $\tilde{V}_0 \gg 1$.

and stretched by the interfacial frictional shear stresses (i.e. for $-a \leq x < 0$). However, for $\tilde{V}_0\tilde{\tau} \ll 1$ and $0 \ll \theta \lesssim \pi/2$, both these terms vanish as the no viscoelastic creep occurs in the adhered sliding portion of the tape (i.e. the tape response is governed by E_0 , see Eq. (21)) and the term $\cos^2\theta \rightarrow 0$ (i.e. the work done by frictional shear stress is negligible, see Eq. (15)). Therefore, under these conditions, even in the case of frictionally sliding interfaces, the only source of the energy dissipation is the viscoelastic creep occurring in the detached tape, which can be quantified as D_f through Eq. (22). Since $D_f = (1 - \cos\theta)^2 D_s < D_s$, for $\theta < \pi/2$, a lower peeling force is predicted in the frictional sliding case compared to stuck interfaces, as indeed shown in Fig. 4. Notably, the effect of the energy dissipation term D_f on the overall peeling behavior can be appreciated by comparing the low speed viscoelastic case (red curve) against the elastic limit (black continuous curve). As already discussed in commenting Eq. (21), a physical explanation of this phenomenon can be found by observing that, in the case of frictional sliding interfaces, the step change occurring in the tape stress at the peeling front is lower than in the case of stuck interfaces, as in the former case the tape in the adhered portion close to the peeling front is pre-stressed by the frictional shear stress by a quantity $\sigma_0 \cos\theta$. Thus, since for $\tilde{V}_0\tilde{\tau} < 1$ the tape pre-stress occurs at a very low excitation frequency (i.e. the tape response does not present any creep), the resulting energy dissipation due to the viscoelastic creep (only occurring in the detached strip) is smaller for frictional sliding interfaces compared to the stuck case, in turn leading to smaller peeling forces.

Figure 5 shows the dimensionless peeling stress $\tilde{\sigma}_0$ as a function of the dimensionless parameter $\tilde{V}_0\tilde{\tau}$ for a given value of θ . All the cases refer to $\tilde{V}_0 > 1$. As expected three different regimes can be observed depending on the value of $\tilde{V}_0\tilde{\tau}$. For $\tilde{V}_0\tilde{\tau} \ll 1$ an asymptotic plateau for $\tilde{\sigma}_0$ is observed as predicted by Eq. (21), which depends on the value of κ . For $\tilde{V}_0\tilde{\tau} \gg 1$, the peeling behavior is governed by Eq. (20) and depends on the high frequency viscoelastic modulus E_∞ . Again, a plateau is observed for $\tilde{\sigma}_0$, whose value saturates as for $\kappa \rightarrow \infty$ as the Rivlin's solution is approached in the case of infinitely stiff tapes. At intermediate values of $\tilde{V}_0\tilde{\tau}$ the hysteretic viscoelastic behavior of the tape plays a key role so

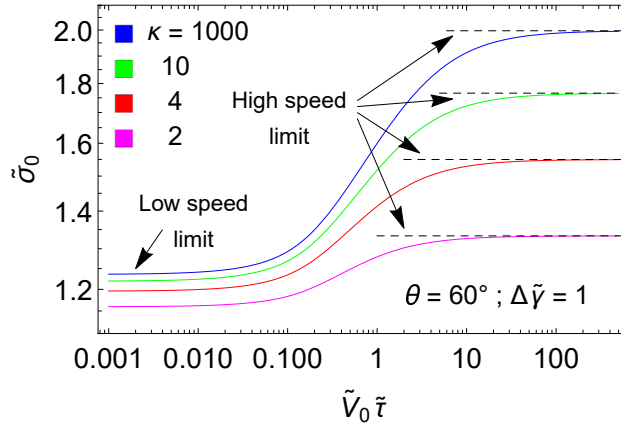


FIG. 5: The dimensionless peeling stress $\tilde{\sigma}_0$ as a function of the dimensionless parameter $\tilde{V}_0 \tilde{\tau}$, for different values of the parameter $\kappa = E_\infty/E_0$. In the figure, both the high and low speed plateau are highlighted. Results refer to $\tilde{V}_0 \gg 1$.

that, in this transition region, the peeling force increases with the peeling rate by following a power law $\tilde{\sigma}_0 \approx (\tilde{V}_0 \tilde{\tau})^n$ where the exponent n depends on the parameter κ .

IV. CONCLUSIONS

In this study, we investigate the peeling behavior of a thin viscoelastic tape peeled away from a rigid substrate. Specifically, we consider two alternative scenarios: one, with the interface between the tape and the rigid substrate under stuck adhesion (i.e. no sliding occurs); the other, assuming relative sliding on a portion of the interface in the presence of frictional shear stresses.

We found that, in stuck interfaces, the overall viscoelastic peeling behavior is independent of the peeling velocity, provided that the peeling velocity $V_0 \gg d/t_c$ (where d is the thickness of the tape and t_c is the creep characteristic time of the viscoelastic material), and the peeling force takes the value predicted by Kendall's peeling model with the elastic modulus given by the high-frequency viscoelastic modulus E_∞ of the tape material. Under these conditions, the energy dissipation associated with the viscoelastic creep of the tape is entirely localized in the detached portion of the tape.

In the presence of frictional sliding at the interface additional sources of energy dissipation come into play, which are associated with both the work done by frictional shear stress and the viscoelastic hysteresis occurring in the portion of the adhering tape subjected to frictional shear stresses. In such conditions, the peeling force is predicted to continuously increase as the peeling angle is decreased, leading to unbounded value for a vanishing peeling angle. Also, the viscoelastic hysteretic behavior of the tape strongly affects the dependence of the peeling force on the peeling velocity. Indeed, for any given value of the peeling angle, three regions can be identified: (i) the low velocity region, where a low plateau is reported for the peeling force; (ii) the transition region, where the peeling force increases as a power law of the peeling velocity, and (iii) the high velocity region, where a high plateau of the peeling force occurs.

Acknowledgement 1 *This project has received funding from the European Union’s Horizon 2020 research and innovation programme under the Marie Skłodowska- Curie grant agreement no. 845756 (N.M. Individual Fellowship). This work was partly supported by the Italian Ministry of Education, University and Research under the Programme “Progetti di Rilevante Interesse Nazionale (PRIN)”, Grant Protocol 2017948, Title: Foam Airless Spoked Tire – FASTire (G.C.)*

- [1] Hyun, S., Pei, L., Molinari, J.F., Robbins, M.O., 2004. Finite-element analysis of contact between elastic self-affine surfaces, *Phys. Rev. E* 2004;70.
- [2] Campana, C., Mueser, M.H., Robbins, M.O., 2008. Elastic contact between self-affine surfaces: comparison of numerical stress and contact correlation functions with analytic predictions. *J. Phys. Condens. Matter* 2008;20(35).
- [3] Yang, C., Persson, B., 2008. Contact mechanics: contact area and interfacial separation from small contact to full contact. *J. Phys.: Condens. Matter* 20 215214.
- [4] Pastewka, L., Robbins, M.O., 2016. Contact area of rough spheres: Large scale simulations and simple scaling laws. *Appl. Phys. Lett.* 108, 221601. <https://doi.org/10.1063/1.4950802>.
- [5] Menga, N., Afferrante, L., Carbone, G, 2016. Adhesive and adhesiveless contact mechanics of elastic layers on slightly wavy rigid substrates. *International Journal of Solids and Structures* 2016;88:101-109. <https://doi.org/10.1016/j.ijstr.2016.03.016>.
- [6] Müser, M., Dapp, W.B., Bugnicourt, R., Sainsot, P., Lesaffre, N., Lubrecht, T., Persson, B., Harris, K.L., Bennett, A., Schulze, K., Rohde, S., Ifju, P., Sawyer, W., Angelini, T., Esfahani, H.A., Kadkhodaei, M., Akbarzadeh, S., Wu, J., Vorlaufer, G., Vernes, A., Solhjoo, S., Vakis, A.I., Jackson, R., Xu, Y., Streater, J., Rostami, A., Dini, D., Medina, S., Carbone, G., Bottiglione, F., Afferrante, L., Monti, J.M., Pastewka, L., Robbins, M., & Greenwood, J., 2017. Meeting the Contact-Mechanics Challenge. *Tribology Letters*, 65, 1-18.
- [7] Menga, N., Carbone, G., 2019. The surface displacements of an elastic half-space subjected to uniform tangential tractions applied on a circular area. *European Journal of Mechanics-A/Solids*, 73, 137-143.
- [8] Menga, N., 2019. Rough frictional contact of elastic thin layers: The effect of geometric coupling. *International Journal of Solids and Structures*, 164, 212-220.
- [9] Persson, B.N.J., 2001. Theory of rubber friction and contact mechanics, *Journal of Chemical Physics* 2001;115:3840 -3861.
- [10] Persson, B.N.J., Albohr, O., Creton, C., Peveri, V., 2004. Contact area between a viscoelastic solid and a hard, randomly rough, substrate. *The Journal of chemical physics*, 120(18), 8779-8793.
- [11] Scaraggi, M., & Persson, B. N. J. (2015). Friction and universal contact area law for randomly rough viscoelastic contacts. *Journal of Physics: Condensed Matter*, 27(10), 105102.
- [12] Menga, N., Putignano, C., Carbone, G., Demelio, G.P., 2014. The sliding contact of a rigid wavy surface with a viscoelastic half-space. *Proc. R. Soc. A*, 470(2169), 20140392.
- [13] Menga, N., Afferrante, L., Carbone, G., 2016. Effect of thickness and boundary conditions on the behavior of viscoelastic layers in sliding contact with wavy profiles. *The Journal of the Mechanics and Physics of Solids* 2016;95: 517-529.

- [14] Menga, N., Afferrante, L., Demelio, G. P., Carbone, G., 2018. Rough contact of sliding viscoelastic layers: numerical calculations and theoretical predictions. *Tribology International*, 122, 67-75.
- [15] Zhang, X., Wang, Q. J., He, T., 2020. Transient and steady-state viscoelastic contact responses of layer-substrate systems with interfacial imperfections. *Journal of the Mechanics and Physics of Solids*, 145, 104170.
- [16] Menga, N., Carbone, G., Dini, D., 2021. Exploring the effect of geometric coupling on friction and energy dissipation in rough contacts of elastic and viscoelastic coatings. *Journal of the Mechanics and Physics of Solids*, 148, 104273.
- [17] Carbone, G., Mangialardi, L., 2008. Analysis of the adhesive contact of confined layers by using a Green's function approach. *Journal of the Mechanics and Physics of Solids*, 56(2), 684-706.
- [18] Martina, D., Creton, C., Damman, P., Jeusette, M., Lindner, A., 2012. Adhesion of soft viscoelastic adhesives on periodic rough surfaces. *Soft Matter*, 8(19), 5350-5357.
- [19] Pastewka, L., Robbins, M.O., 2014. Contact between rough surfaces and a criterion for macroscopic adhesion. *Proceedings of the National Academy of Sciences*, 111(9), 3298-3303.
- [20] Medina S., Dini D., 2014. A numerical model for the deterministic analysis of adhesive rough contacts down to the nano-scale. *International Journal of Solids and Structures*, 51(14):2620-2632.
- [21] Rey, V., Anciaux, G., Molinari, J.F., 2017. Normal adhesive contact on rough surfaces: efficient algorithm for FFT-based BEM resolution. *Computational Mechanics*, 60(1), 69-81.
- [22] Menga, N., Carbone, G., Dini, D., 2018. Do uniform tangential interfacial stresses enhance adhesion? *Journal of the Mechanics and Physics of Solids*, 112:145-156.
- [23] Menga, N., Carbone, G., Dini, D., 2019. Corrigendum to: "Do uniform tangential interfacial stresses enhance adhesion?". *Journal of the Mechanics and Physics of Solids*, 133:103744. Doi: <https://doi.org/10.1016/j.jmps.2019.103744>
- [24] Menga, N., Putignano, C., Afferrante, L., Carbone, G., 2019. The Contact Mechanics of Coated Elastic Solids: Effect of Coating Thickness and Stiffness. *Tribology Letters*, 67(1), 24.
- [25] Zhu, Z., Xia, Y., Jiang, C., Yang, Z., Jiang, H., 2021. Investigation of zero-degree peeling behavior of visco-hyperelastic highly stretchable adhesive tape on rigid substrate. *Engineering Fracture Mechanics*, 241, 107368.
- [26] Creton, C., Ciccotti, M., 2016. Fracture and adhesion of soft materials: a review. *Reports on Progress in Physics*, 79(4), 046601.
- [27] Kendall, K., 1975. Thin-film peeling-the elastic term. *J. Phys. D: Appl Phys* 8, 1449-1452.
- [28] Kendall, K., 1973. Peel adhesion of solid films-the surface and bulk effects. *The Journal of Adhesion*, 5(3), 179-202.
- [29] Kendall, K., 1973. The shapes of peeling solid films. *The Journal of Adhesion*, 5(2), 105-117.
- [30] Afferrante, L., Carbone, G., 2016. The ultratough peeling of elastic tapes from viscoelastic substrates. *Journal of the Mechanics and Physics of Solids*, 96, 223-234.
- [31] Pierro, E., Afferrante, L., Carbone, G., 2020. On the peeling of elastic tapes from viscoelastic substrates: Designing materials for ultratough peeling. *Tribology International*, 146, 106060.
- [32] Derail, C., Allal, A., Marin, G., Tordjeman, P., 1997. Relationship between viscoelastic and peeling properties of model adhesives. Part 1. Cohesive fracture. *The Journal of Adhesion*, 61(1-4), 123-157.
- [33] Zhou, M., Tian, Y., Pesika, N., Zeng, H., Wan, J., Meng, Y., Wen, S., 2011. The extended peel zone model: effect of peeling velocity. *The Journal of Adhesion*, 87(11), 1045-1058.

- [34] Chen, H., Feng, X., Huang, Y., Huang, Y., Rogers, J.A., 2013. Experiments and viscoelastic analysis of peel test with patterned strips for applications to transfer printing. *Journal of the Mechanics and Physics of Solids*, 61(8), 1737-1752.
- [35] Peng, Z., Wang, C., Chen, L., Chen, S., 2014. Peeling behavior of a viscoelastic thin-film on a rigid substrate. *International Journal of Solids and Structures*, 51(25-26), 4596-4603.
- [36] Kendall, K., 1975. Crack propagation in lap shear joints. *Journal of Physics D: Applied Physics*, 8(5), 512.
- [37] Kendall, K., 1978. Interfacial dislocations spontaneously created by peeling.(Adhesive joint strength). *Journal of Physics D: Applied Physics*, 11(11), 1519.
- [38] Newby, B.M.Z., Chaudhury, M.K., Brown, H.R., 1995. Macroscopic evidence of the effect of interfacial slippage on adhesion. *Science*, 269(5229), 1407-1409.
- [39] Zhang Newby, B.M., Chaudhury, M.K., 1997. Effect of interfacial slippage on viscoelastic adhesion. *Langmuir*, 13(6), 1805-1809.
- [40] Wang, S.J., Li, X., 2007. The effects of tensile residual stress and sliding boundary on measuring the adhesion work of membrane by pull-off test. *Thin solid films*, 515(18), 7227-7231.
- [41] Begley, M.R., Collino, R.R., Israelachvili, J.N., McMeeking, R.M., 2013. Peeling of a tape with large deformations and frictional sliding. *Journal of the Mechanics and Physics of Solids*, 61(5), 1265-1279.
- [42] Autumn, K., Hsieh, S., Dudek, D., Chen, J., Chitaphan, C., Full, R.J., 2006. Dynamics of geckos running vertically. *J. Exp. Biol.* 209, 260–272. doi:10.1242/jeb.01980.
- [43] Autumn, K., Dittmore, A., Santos, D., Spenko, M., Cutkosky, M., 2006. Frictional adhesion: a new angle on gecko attachment. *Journal of Experimental Biology*, 209(18), 3569-3579.
- [44] Tian, Y., Pesika, N., Zeng, H., Rosenberg, K., Zhao, B., McGuiggan, P., Autumn, K., Israelachvili, J., 2006. Adhesion and friction in gecko toe attachment and detachment. *Proc. Natl Acad. Sci. USA* 103, 19 320–19 325. doi:10.1073/pnas.0608841103.
- [45] Endlein, T., Federle, W., 2013. Rapid reflexes in smooth adhesive pads of insects prevent sudden detachment. *Proc. R. Soc. B* 280, 20122868. doi:10.1098/rspb.2012.2868.
- [46] Labonte, D., Federle, W., 2015. Rate-dependence of ‘wet’ biological adhesives and the function of the pad secretion in insects. *Soft Matter* 11, 8661–8673. doi:10.1039/C5SM01496D.
- [47] Endlein, T., Ji, A., Samuel, D., Yao, N., Wang, Z., Barnes, W.J.P., Federle, W., Kappl, M., Dai, Z., 2013. Sticking like sticky tape: tree frogs use friction forces to enhance attachment on overhanging surfaces. *J. R. Soc. Interface* 10, 20120838. doi:10.1098/rsif.2012.0838.
- [48] Gao, H., Wang, X., Yao, H., Gorb, S., Arzt, E., 2005. Mechanics of hierarchical adhesion structures of geckos. *Mechanics of Materials*, 37(2-3), 275-285.
- [49] Lee, D.Y., Lee, D.H., Lee, S.G., & Cho, K., 2012. Hierarchical gecko-inspired nanohairs with a high aspect ratio induced by nanoyielding. *Soft Matter*, 8(18), 4905-4910.
- [50] Zhao, H.P., Wang, Y., Li, B. W., Feng, X.Q., 2013. Improvement of the peeling strength of thin films by a bioinspired hierarchical interface. *International Journal of Applied Mechanics*, 5(02), 1350012.
- [51] Heepe, L., Raguseo, S., Gorb, S.N., 2017. An experimental study of double-peeling mechanism inspired by biological adhesive systems. *Applied Physics A*, 123(2), 124.
- [52] Menga, N., Afferrante, L., Pugno, N. M., Carbone, G., 2018. The multiple V-shaped double peeling of elastic thin films from elastic soft substrates. *Journal of the Mechanics and Physics of Solids*, 113, 56-64.
- [53] Menga, N., Dini, D., Carbone, G., 2020. Tuning the periodic V-peeling behavior of elastic tapes applied to thin compliant substrates. *International Journal of Mechanical Sciences*, 170,

105331.

- [54] Afferrante, L., Carbone, G., Demelio, G., Pugno, N., 2013. Adhesion of elastic thin films: double peeling of tapes versus axisymmetric peeling of membranes. *Tribology Letters*, 52(3), 439-447.
- [55] Labonte, D., Federle, W., 2016. Biomechanics of shear-sensitive adhesion in climbing animals: peeling, pre-tension and sliding-induced changes in interface strength. *Journal of The Royal Society Interface*, 13(122), 20160373.
- [56] Chen, B., Wu, P., Gao, H., 2009. Pre-tension generates strongly reversible adhesion of a spatula pad on substrate. *J. R. Soc. Interface* 6, 529–537. doi:10. 1098/rsif.2008.0322.
- [57] Williams, J., 1993. A review of the determination of energy release rates for strips in tension and bending. Part I—static solutions. *J. Strain Anal. Eng.* 28, 237–246. doi:10.1243/03093247V284237.
- [58] Amouroux, N., Petit, J., Le´ger, L., 2001. Role of interfacial resistance to shear stress on adhesive peel strength. *Langmuir* 17, 6510–6517. doi:10. 1021/la010146r.
- [59] Federle, W., Riehle, M., Curtis, A.S., Full, R.J., 2002. An integrative study of insect adhesion: mechanics and wet adhesion of pretarsal pads in ants. *Integrative and Comparative Biology*, 42(6), 1100-1106.
- [60] Federle, W., Baumgartner, W., Hölldobler, B., 2004. Biomechanics of ant adhesive pads: frictional forces are rate-and temperature-dependent. *Journal of Experimental Biology*, 207(1), 67-74.
- [61] Gorb, S., Jiao, Y., Scherge, M., 2000. Ultrastructural architecture and mechanical properties of attachment pads in *Tettigonia viridissima* (Orthoptera Tettigoniidae). *Journal of Comparative Physiology A*, 186(9), 821-831.
- [62] Puthoff, J.B., Holbrook, M., Wilkinson, M.J., Jin, K., Pesika, N.S., Autumn, K., 2013. Dynamic friction in natural and synthetic gecko setal arrays. *Soft Matter*, 9(19), 4855-4863.
- [63] Carbone, G., Persson, B.N.J., 2005. "Hot cracks in rubber: origin of the giant toughness of rubberlike materials." *Physical review letters* 95.11 (2005): 114301
- [64] Carbone, G., Persson, B.N.J., 2005. Crack motion in viscoelastic solids: the role of the flash temperature. *The European Physical Journal E*, 17(3), 261-281
- [65] Christensen, R.M., 1982. *Theory of viscoelasticity*, Academic Press, New York.
- [66] Lin, Y., Freund, L.B., 2007. Forced detachment of a vesicle in adhesive contact with a substrate. *International journal of solids and structures*, 44(6), 1927-1938.
- [67] Collino, R.R., Philips, N.R., Rossol, M.N., McMeeking, R.M., Begley, M.R., 2014. Detachment of compliant films adhered to stiff substrates via van der Waals interactions: role of frictional sliding during peeling. *Journal of The Royal Society Interface*, 11(97), 20140453.
- [68] Jagota, A., Hui, C.Y., 2011. Adhesion, friction, and compliance of bio-mimetic and bio-inspired structured interfaces. *Materials Science and Engineering: R: Reports*, 72(12), 253-292.